

Momentum Distribution of a Fermi Gas of Atoms in the BCS-BEC Crossover

C. A. Regal,^{1,*} M. Greiner,¹ S. Giorgini,^{1,2} M. Holland,¹ and D. S. Jin¹

¹JILA, Quantum Physics Division, National Institute of Standards and Technology and University of Colorado, Boulder, Colorado 80309-0440, USA

and Department of Physics, University of Colorado, Boulder, Colorado 80309-0440, USA

²Dipartimento di Fisica, Università di Trento and BEC-INFN, I-38050 Povo, Italy

(Received 12 July 2005; published 16 December 2005)

We observe dramatic changes in the atomic momentum distribution of a Fermi gas in the crossover region between the BCS theory superconductivity and Bose-Einstein condensation (BEC) of molecules. We study the shape of the momentum distribution and the kinetic energy as a function of interaction strength. The momentum distributions are compared to a mean-field crossover theory, and the kinetic energy is compared to theories for the two weakly interacting limits. This measurement provides a unique probe of pairing in a strongly interacting Fermi gas.

DOI: 10.1103/PhysRevLett.95.250404

PACS numbers: 03.75.Ss, 05.30.Fk

Recent years have seen the emergence of an intriguing Fermi system achieved with ultracold gases of ⁴⁰K or ⁶Li atoms. With these systems it is possible to widely tune the interatomic interaction strength, represented dimensionlessly as $k_F a$, where k_F is the Fermi wave vector and a is the scattering length. Of particular interest is the strongly interacting regime ($-1 < 1/k_F a < 1$) where a crossover between the BCS theory of superconductivity and Bose-Einstein condensation (BEC) of molecules occurs [1–3]. Experimental probes have been numerous and have shown, for example, that these Fermi systems cross a phase transition as a function of temperature [4,5] and display features of the BCS-BEC crossover such as a pairing gap Δ , on the order of the Fermi energy E_F [6].

One classic phenomenon associated with pairing in a Fermi system that has yet to be explored fully in atomic systems is a broadening of the Fermi surface in momentum space (see for example Ref. [7]). Figure 1 (inset) shows the expected momentum distribution of a homogeneous, zero temperature ($T = 0$) Fermi system. In the BCS limit ($1/k_F a \rightarrow -\infty$) the amount of broadening is small and associated with Δ . As the interaction increases this effect grows until at unitarity ($1/k_F a = 0$) the effect is on order of E_F , and in the BEC limit ($1/k_F a \rightarrow \infty$) the momentum distribution becomes the square of the Fourier transform of the molecule wave function (see for example Ref. [8]).

In this Letter we present a measurement of the atom momentum distribution of a trapped Fermi gas in the BCS-BEC crossover regime. In the strongly interacting regime this measurement probes the pair wave function and consequently the nature of the pairs: Small, tightly bound pairs will broaden the momentum distribution more than a large, weakly bound pair. Similarly a fully paired gas will broaden the distribution more than a gas with a small number of paired atoms. It is expected that this measurement, while probing the nature of the pairs, will not be sensitive to coherence between pairs. While in the BCS limit the pairs are always coherent, when the interaction

becomes large so-called preformed pairs are predicted to form above the phase transition temperature T_c [1,9]. To verify such theories it is important that techniques for detecting pairing, such as this result and those in Refs. [6,10,11], be developed alongside the more numerous studies probing the phase transition [4,5,12–16].

To perform the experiment we prepare a ⁴⁰K gas near a scattering resonance known as a Feshbach resonance, where we can tune the s -wave interaction between fermions by varying the magnetic field B [17,18]. To probe the

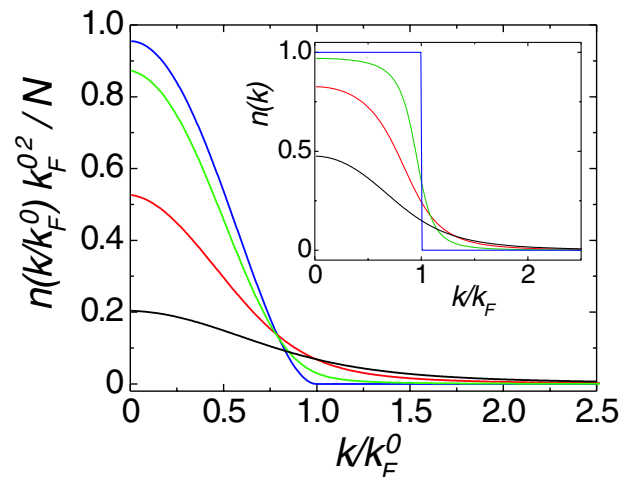


FIG. 1 (color online). Theoretical column integrated momentum distributions of a trapped Fermi gas $n(k)$ calculated from a mean-field theory [21]. N is the total particle number; k_F^0 is the noninteracting Fermi wave vector. The normalization is given by $2\pi \int n(k) k dk = N$, and we note that the normalization is strongly affected by the tail of the distribution. The lines correspond to various values of $1/k_F^0 a$, with the tallest curve (blue online) representing $a = 0$ and the broadest curve (black online) representing $1/k_F^0 a = 0.59$. The middle curves correspond to $1/k_F^0 a = -0.66$ (green online) and $1/k_F^0 a = 0$ (red online). Inset: Corresponding distributions for a homogeneous system.

system we use the standard technique of time-of-flight expansion followed by absorption imaging [19]. To measure the momentum distribution of atoms the gas must expand freely without any interatomic interactions; to achieve this we quickly change the scattering length to zero for the expansion. Bourdel *et al.* pioneered this type of measurement using a gas of ${}^6\text{Li}$ atoms at $T/T_F \approx 0.6$, where T_F is the Fermi temperature [20]. Here we report measurements at $T/T_F \approx 0.1$, where pairing becomes a significant effect and condensates have been observed [4,5].

To understand what we expect for our trapped atomic system, we can predict the atomic momentum distribution using a local density approximation and the results for the homogeneous case. In the trapped gas case, in addition to the local broadening of the momentum distribution due to pairing, attractive interactions compress the density profile and thereby enlarge the overall momentum distribution. Figure 1 shows an integrated column density from the result of a mean-field calculation at $T = 0$ as described in Refs. [21,22].

In our experimental setup we create an ultracold ${}^{40}\text{K}$ gas using previously described cooling techniques [17,24]. The gas is prepared in a nearly equal mixture of the spin states $|f, m_f\rangle = |9/2, -9/2\rangle$ and $|9/2, -7/2\rangle$, where f is the total spin and m_f the spin-projection quantum number. The final ultracold gas is held in an optical dipole trap formed at the intersection of two Gaussian laser beams. One beam is oriented parallel to the force of gravity (\hat{y}) with a waist of $w_y = 200 \mu\text{m}$ and the second beam is perpendicular to the first (\hat{z}) and has $w_z = 15 \mu\text{m}$.

In this Letter we have measured the atomic momentum distribution with a low temperature Fermi gas. We start with a weakly interacting gas at $T = 0.12T_F$ in a trap with a radial frequency of $\nu_r = 280 \text{ Hz}$ and an aspect ratio of $\nu_z/\nu_r = 0.071$. We then adiabatically increase the interaction strength by ramping the magnetic field at a rate of $(6.5 \text{ ms/G})^{-1}$ to near a Feshbach resonance located at $202.10 \pm 0.07 \text{ G}$ [4]. After a delay of 1 ms, both dipole trap beams are switched off and simultaneously a magnetic-field ramp to $a \approx 0$ ($B = 209.6 \text{ G}$) at a rate of $(2 \mu\text{s/G})^{-1}$ is initiated. The rate of this magnetic-field ramp is designed to be fast compared to typical many-body time scales as determined by $\frac{\hbar}{E_F} = 90 \mu\text{s}$. The cloud is allowed to freely expand for 12.2 ms, and then an absorption image is taken. The imaging beam propagates along \hat{z} and selectively probes the $|9/2, -9/2\rangle$ state [17].

Samples of these absorption images, azimuthally averaged, are shown in Fig. 2 for various values of $1/k_F^0 a$, where the superscript 0 indicates a quantity that was measured in the weakly interacting regime. We observe a dramatic change in the distribution as predicted in Fig. 1. Some precautions need to be taken in quantitative comparison of Figs. 1 and 2. First, the magnetic-field ramp to the Feshbach resonance, while adiabatic with respect to most time scales, is not fully adiabatic with respect to the axial trap period. Second, in the experiment an adiabatic

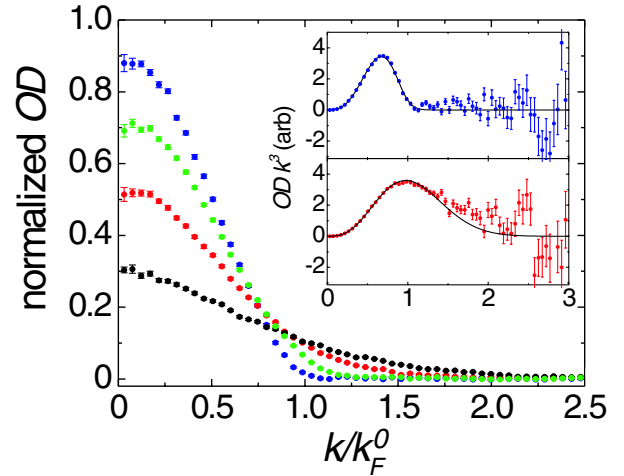


FIG. 2 (color online). Experimental, azimuthally averaged, momentum distributions of a trapped Fermi gas normalized such that the area under the curves is the same as in Fig. 1. The curves, in order of highest to lowest maximum OD, correspond to the following values of $1/k_F^0 a$: -71 (blue online), -0.66 (green online), 0 (red online), and 0.59 (black online). Error bars represent the standard deviation of the mean of averaged pixels. Inset: Curves for $1/k_F^0 a = -71$ (top) and 0 (bottom) weighted by k^3 . The lines are the results of a fit to Eq. (1).

field ramp keeps the entropy of the gas, not T/T_F , constant. However, we expect the resulting change in T/T_F to have a minimal effect on the distribution for $1/k_F^0 a < 0$ [25]. Third, the theory assumes $T = 0$ and does not include the Hartree term, thus underestimating the broadening on the BCS side compared to a full theory [23].

It is natural now to consider extracting the kinetic energy from the momentum distribution. While the momentum distribution should be universal for small momenta, for large momenta it is influenced by details of the interatomic scattering potential. In the extreme case of a delta potential, which we used for the calculation in Fig. 1, the momentum distribution has a tail with a $1/k^4$ dependence, giving rise to a divergence of the kinetic energy. In the experiment we avoid a dependence of the measured kinetic energy on details of the interatomic potential because our magnetic-field ramp is never fast enough to access features on order of the interaction length of the van der Waals potential, $r_0 \approx 60a_0$ for ${}^{40}\text{K}$ [26]. Thus, the results presented in this Letter represent a universal quantity, independent of the details of the interatomic potential. Although universal in this sense, the measured kinetic energy is intrinsically dependent on the dynamics of the magnetic-field ramp, with faster ramps corresponding to higher measured energies.

To obtain the kinetic energy from the experimental data exactly we would need to take the second moment of the distribution, which is proportional to $\sum k^3 \text{OD} / \sum k \text{OD}$, where OD is the optical depth. As illustrated in Fig. 2 (inset) this is difficult due to the decreased signal-to-noise ratio for large k . Thus, our approach will be to apply a 2D

surface fit to the image and extract an energy from the fitted function. In the limit of weak interactions the appropriate function is that for an ideal, harmonically trapped Fermi gas. This is

$$\text{OD}(x, y) = pk g_2(-\zeta e^{-(x^2/2\sigma_x^2)-(y^2/2\sigma_y^2)})/g_2(-\zeta) \quad (1)$$

where $g_n(x) = \sum_{k=1}^{\infty} \frac{x^k}{k^n}$, ζ is the fugacity, $\sigma_{x,y}^2$ are proportional to the Fermi gas temperature, and pk is the maximum OD. The kinetic energy per particle is then given by

$$E_{\text{kin}} = \frac{3}{2} \frac{m\sigma_x\sigma_y}{t^2} \frac{g_4(-\zeta)}{g_3(-\zeta)} \quad (2)$$

where m is the mass of ^{40}K and t is the expansion time [27]. Although Eq. (1) is not an accurate theoretical description of the Fermi gas in the crossover, empirically we find it is a fitting function that describes the data reasonably well throughout the crossover, as illustrated in Fig. 2 (inset).

Figure 3 shows the result of extracting E_{kin} as a function of $1/k_F^0 a$; we see that E_{kin} more than doubles between the noninteracting regime and unitarity. We have checked that heating and loss due to inelastic processes are negligible up to $1/k_F^0 a \sim 0$. To do this we performed an experiment in which we adiabatically approached the Feshbach resonance at rate of $(6 \text{ ms/G})^{-1}$, waited 1 ms, and then ramped back at the same slow rate to the weakly interacting regime

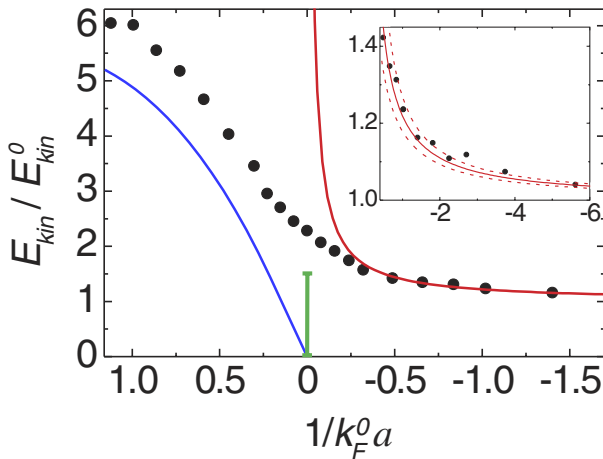


FIG. 3 (color online). The points (●) show the measured energy E_{kin} normalized to $E_{\text{kin}}^0 = 0.25k_b \mu\text{K}$ ($E_{\text{kin}}^0 = \frac{3}{8}E_F$ for a harmonically trapped gas at $T = 0$). The solid curve above the points (red online) is the expected energy ratio from a calculation only valid in the weakly interacting regime ($1/k_F^0 a < -1$). In the strongly interacting regime pairing due to many-body effects strongly increases E_{kin} . The vertical bar (green online) represents the expected value of $E_{\text{kin}}/E_{\text{kin}}^0$ at unitarity just due to density profile rescaling (see text). In the molecule limit ($1/k_F^0 a > 1$) we calculate the expected energy for an isolated molecule [curve below the points (blue online)]. Inset: A focus on the weakly interacting regime with the same axes definitions as the main graph. The dashed lines show the uncertainty in the calculation based upon the uncertainty in the Feshbach resonance parameters [4,18].

regime. If we start with a cloud initially at $T/T_F = 0.10$, T/T_F upon return increases by less than 10% for a ramp to $1/k_F^0 a = 0$ (yet by 80% for a ramp to $1/k_F^0 a = 0.5$).

Using the fitting function of Eq. (1) we can also extract information about the shape of the distribution through the parameter ζ . Since ζ can range from -1 to ∞ it is convenient to plot the quantity $\ln(1 + \zeta)$ (Fig. 4). The fit reveals that the shape evolves smoothly from that of an ideal Fermi gas at $T/T_F \sim 0.1$ in the weakly interacting regime, to a Gaussian near unitarity, and to a shape more peaked than a Gaussian in the BEC regime. These qualitative features are predicted by the mean-field calculation of the distributions in Fig. 1.

As mentioned earlier E_{kin} of a trapped gas is affected both by the broadening due to pairing [Fig. 1 (inset)] and by changes in the trapped gas density profile. In the BCS limit, the broadening due to pairing scales with $e^{-\pi/2k_F^0|a|}$ and is thus exponentially small compared to density profile changes, which scale linearly with $k_F^0|a|$. In this limit we can calculate $E_{\text{kin}}/E_{\text{kin}}^0$ using a mean-field calculation in the normal state [28] to find, to lowest order in $k_F^0|a|$, $E_{\text{kin}}/E_{\text{kin}}^0 = \frac{2048}{945\pi^2} k_F^0|a| + 1$. We plot this result in Fig. 3 (inset) and find good agreement for the weakly interacting regime ($1/k_F^0 a < -1$). However, caution must be taken with the apparent agreement for $-0.5 < 1/k_F^0 a < -1$. The agreement could be explained by the lack of pairing in this theory being compensated by the theory's overestimation of the density profile change when $|a|$ becomes larger than $1/k_F$.

In the crossover regime where the pairs are more tightly bound, pairing provides a significant contribution to the change in the momentum distribution. At unitarity a full Monte Carlo calculation predicts the radius of the Fermi gas density profile to become $(1 + \beta)^{1/4} R_0 = 0.81 R_0$, where R_0 is the Thomas-Fermi radius of a noninteracting Fermi gas [23]. Just this rescaling would result in $E_{\text{kin}}/E_{\text{kin}}^0 = 1.54$ [vertical (green online) bar in Fig. 3]. Thus, at unitarity, pairing effects on the momentum distribution must account for a large fraction of the measured

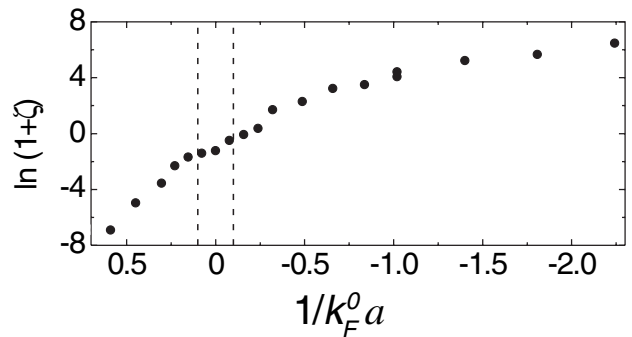


FIG. 4. Shape of the momentum distribution as described through the parameter ζ [Eq. (1)]. $\ln(1 + \zeta) = 0$ corresponds to a Gaussian distribution, and for an ideal Fermi gas $\ln(1 + \zeta)^{-1} \approx T/T_F$ in the limit of low T/T_F . The dashed lines show the uncertainty in the Feshbach resonance position [4].

value of $E_{\text{kin}}/E_{\text{kin}}^0 = 2.3 \pm 0.3$ (Fig. 3) and all of the observed change in distribution shape (Fig. 4).

In the BEC limit we expect the measured energy to be that of an isolated diatomic molecule after dissociation by the magnetic-field ramp. Provided the scattering length associated with the initial molecular state, $a(t=0)$, is much larger than $r_0 \approx 60a_0$, the wave function for the molecule is given by $\psi = Ae^{-r/a(t=0)}/r$ where r is the internuclear separation and A is a normalization constant. We can calculate the measured energy from the solution of the Schrödinger equation with a time-dependent boundary condition on the two-particle wave function $\frac{d \log(r\psi)}{dr} \Big|_{r=0} = -\frac{1}{a(t)}$, where $a(t)$ is the scattering length fixed by the magnetic field at time t . In Fig. 3 we show the result of this calculation for a pure gas of molecules and a $(2 \mu\text{s/G})^{-1}$ ramp rate. We find reasonable agreement considering that there is a large systematic uncertainty in the theory curve due to the experimental uncertainty in the magnetic-field ramp rate and that this two-body theory should match the data only in the BEC limit ($1/k_F^0 a \gg 1$).

We have found that the momentum distribution of a Fermi gas provides a wealth of information on crossover physics. The measurement is a probe of pairing in the strongly interacting regime. It provides a universal thermodynamic quantity that, like previously measured energies in the BCS-BEC crossover [14,17,20,29,30], has the potential to provide a stringent test for crossover theories. A theory that correctly describes the momentum distributions measured in this Letter must be able to properly treat dynamics. Recent results also suggest that the simple Nozieres-Schmitt-Rink ground state [8] will not accurately reproduce the kinetic energy in the strongly interacting regime (Fig. 3) [31]. Thus, the data could help test more sophisticated crossover theories (for example, Ref. [23]). Lastly, we note that this work also provides a starting point for future experiments seeking to probe pair correlations in the momentum distribution using measurements of atom shot noise [32,33].

We thank Q. Chen and K. Levin for valuable discussions and J. T. Stewart for experimental assistance. This work was supported by NSF, NIST, and NASA. C. A. R. acknowledges support from the Hertz Foundation. M. H. acknowledges support from the U.S. Department of Energy, Office of Basic Energy Sciences via the Chemical Sciences, Geosciences and Biosciences Division.

*Email address: regal@jilau1.colorado.edu

[1] M. Randeria, in *Bose-Einstein Condensation*, edited by A. Griffin, D.W. Snoke, and S. Stringari (Cambridge

University, Cambridge, 1995), pp. 355–392, and references therein.

- [2] E. Timmermans, K. Furuya, P.W. Milonni, and A.K. Kerman, *Phys. Lett. A* **285**, 228 (2001).
- [3] M. Holland, S.J.J.M.F. Kokkelmans, M.L. Chiofalo, and R. Walser, *Phys. Rev. Lett.* **87**, 120406 (2001).
- [4] C.A. Regal, M. Greiner, and D.S. Jin, *Phys. Rev. Lett.* **92**, 040403 (2004).
- [5] M.W. Zwierlein *et al.*, *Phys. Rev. Lett.* **92**, 120403 (2004).
- [6] C. Chin *et al.*, *Science* **305**, 1128 (2004).
- [7] P.G. de Gennes, *Superconductivity of Metals and Alloys* (Addison-Wesley, California, 1966).
- [8] P. Nozieres and S. Schmitt-Rink, *J. Low Temp. Phys.* **59**, 195 (1985).
- [9] Q. Chen, J. Stajic, S. Tan, and K. Levin, *Phys. Rep.* **412**, 1 (2005).
- [10] M. Greiner, C.A. Regal, and D.S. Jin, *Phys. Rev. Lett.* **94**, 070403 (2005).
- [11] G.B. Partridge *et al.*, *Phys. Rev. Lett.* **95**, 020404 (2005).
- [12] J. Kinast *et al.*, *Phys. Rev. Lett.* **92**, 150402 (2004).
- [13] M. Bartenstein *et al.*, *Phys. Rev. Lett.* **92**, 203201 (2004).
- [14] T. Bourdel *et al.*, *Phys. Rev. Lett.* **93**, 050401 (2004).
- [15] J. Kinast *et al.*, *Science* **307**, 1296 (2005).
- [16] M. Zwierlein *et al.*, *Nature (London)* **435**, 1047 (2005).
- [17] C.A. Regal and D.S. Jin, *Phys. Rev. Lett.* **90**, 230404 (2003).
- [18] C.A. Regal, C. Ticknor, J.L. Bohn, and D.S. Jin, *Phys. Rev. Lett.* **90**, 053201 (2003).
- [19] M.H. Anderson *et al.*, *Science* **269**, 198 (1995).
- [20] T. Bourdel *et al.*, *Phys. Rev. Lett.* **91**, 020402 (2003).
- [21] L. Viverit, S. Giorgini, L. Pitaevskii, and S. Stringari, *Phys. Rev. A* **69**, 013607 (2004).
- [22] A similar local density calculation at unitarity using the momentum distribution obtained from quantum Monte Carlo simulations shows good agreement with the mean-field result for this observable [23].
- [23] G.E. Astrakharchik *et al.*, *Phys. Rev. Lett.* **93**, 200404 (2004); *Phys. Rev. Lett.* **95**, 230405 (2005).
- [24] B. DeMarco and D.S. Jin, *Science* **285**, 1703 (1999).
- [25] Q. Chen, J. Stajic, and K. Levin, cond-mat/0411090 [*Phys. Rev. Lett.* (to be published)].
- [26] G.F. Gribakin and V.V. Flambaum, *Phys. Rev. A* **48**, 546 (1993).
- [27] This calculation gives the total E_{kin} in all three dimensions. Since the momentum distribution was only measured in two directions, Eq. (2) requires the assumption that the third dimension reveals an identical distribution.
- [28] L. Vichi and S. Stringari, *Phys. Rev. A* **60**, 4734 (1999).
- [29] K.M. O'Hara *et al.*, *Science* **298**, 2179 (2002).
- [30] M. Bartenstein *et al.*, *Phys. Rev. Lett.* **92**, 120401 (2004).
- [31] M.L. Chiofalo, S. Giorgini, and M. Holland (to be published).
- [32] E. Altman, E. Demler, and M.D. Lukin, *Phys. Rev. A* **70**, 013603 (2004).
- [33] M. Greiner, C.A. Regal, J.T. Stewart, and D.S. Jin, *Phys. Rev. Lett.* **94**, 110401 (2005).